JMEPEG (2012) 16:240–246
DOI: 10.1007/s11665-011-9925-0

1059-9495/$19.00

Influence of 2,3-Dihydroxyflavanone on Corrosion Inhibition of Mild Steel in Acidic Medium

M. Gopiraman, C. Sathya, S. Vivekananthan, D. Kesavan, and N. Sulochana

(Submitted September 2, 2010; in revised form March 5, 2011)

The inhibition effect of 2,3-dihydroxyflavone on the corrosion of mild steel in 100-600 ppm aqueous hydrochloric acid solution has been investigated by weight loss and electrochemical impedance spectroscopy. The corrosion inhibition efficiency increases with increasing concentration and time. The effect of temperature on the corrosion behavior of mild steel in 1 M HCl with addition of inhibitor was studied at the temperature range of 300-330 K. UV-Vis, FTIR, and surface analysis (SEM) was also carried out to establish the corrosion inhibitive property of this inhibitor in HCl solution. The adsorption of this inhibitor on the mild steel surface obeys the Langmuir adsorption isotherm. Electrochemical studies reveal that the inhibitor is a cathodic type.

Keywords 2,3-dihydroxyflavanone, corrosion inhibitor, mild steel, SEM

1. Introduction

During the past decade, the inhibition of mild steel in acid solutions by different types of organic inhibitors has been extensively studied (Ref 1-6). Organic compounds containing electronegative functional groups and π electron in triple or conjugated double bonds are usually good inhibitors. Heteroatoms as sulfur, phosphorus, nitrogen, and oxygen as well as aromatic rings in their structure are the major adsorption centers (Ref 7, 8).

The recent trend is toward environment friendly inhibitors. As most of the natural products are nontoxic, biodegradable and readily available in plenty, various parts-seeds, fruits, leaves, flowers, etc., have been used as corrosion inhibitors (Ref 9-11).

The natural products such as 2,3-dihydroxyflavanone have higher electron density at heteroatoms. It has been reported that the biological systems have the corrosion inhibition efficiency due to the functional groups present in aromatic and heterocyclic rings along with electron-rich elements like nitrogen, sulfur, and oxygen. These substances are found to adsorb on the corroding metal surface and reduce the inhibition tendency (Ref 12, 13).

In this study, the inhibition potential of 2,3-dihydroxyflavone in 1 M HCl through weight loss, electrochemical studies, adsorption isotherms, FT-IR spectrum, UV-Visible spectrum, and SEM techniques have been investigated.

M. Gopiraman, C. Sathya, S. Vivekananthan, D. Kesavan, and **N. Sulochana**, Department of Chemistry, National Institute of Technology, Trichy 620015, India; and **D. Kesavan**, Institute of High Polymer Research, Faculty of Textile Science and Technology, Shinshu University, Tokida 3-15-1, Ueda 386-8567, Japan. Contact e-mail: n.sulocha@gmail.com.

2. Experimental

2.1 Weight Loss Method

Mild steel specimens having compositions 0.10% C, 0.34% Mn, 0.08% P, and the remainder being Fe were used. The specimens of dimension 3 cm × 2 cm × 0.28 cm are used. The flavone inhibitor (Fig. 1) had been purchased from Research Organics, Chennai, India. Double-distilled water was used to prepare solutions of analar grade (Merck) 1 M HCl and various concentrations of inhibitor.

Weight loss study was carried out at 300, 310, 320, and 330 K temperatures for 2 h time duration in 1 M HCl solution. From weight loss, inhibition efficiency (IE) was calculated (Ref 14).

The values of activation energy (E_a) were calculated using Arrhenius equation. The free energy of adsorption (ΔG_{ads}) at different temperatures was calculated using the following equation (Ref 15):

$$\Delta G_{ads} = -RT\ln(55.5K) \quad \text{(Eq 1)}$$

and K is given by

$$K = \theta/(1-\theta) \times 1/C \quad \text{(Eq 2)}$$

where θ is degree of coverage on metal surface, C is the concentration in mol, and K is the equilibrium constant. The degree of surface coverage (θ) for optimum concentration of inhibitor in 1 M HCl at 300-330 K for 2 h immersion time has been evaluated from the weight loss values. A plot of log (θ/1 − θ) versus $1/T$ gave a straight line. The value of heat of adsorption (Q) was obtained from the slope of this plot. The values of enthalpy of activation (ΔH) and entropy of activation (ΔS) were calculated using the following equation:

$$\text{Rate} = (RT/N\,h)\exp[(\Delta S/R]\exp[\Delta H/RT] \quad \text{(Eq 3)}$$

where h is the Planck's constant, N the Avogadro number, and R the gas constant. A plot of log (CR/T) versus $1/T$ gave a straight line with a slope of ($-\Delta H/2.303R$) and an intercept of [(log(R/Nh) + ($\Delta S/2.303R$)].

2.2 Electrochemical Studies

CH electrochemical analyzer model 604B was used to record Tafel polarization curve and Nyquist impedance curve. A conventional three-electrode system was used for this purpose. Mild steel specimen of an exposed area of 1 cm^2 was used as a working electrode. Pt and SCE were used as auxiliary and reference electrodes, respectively. The working electrode was polished with 1/0, 2/0, 3/0, and 4/0 grade emery papers and degreased with double-distilled water and acetone before usage. The linear Tafel segments of the anodic and cathodic curves were extrapolated to the corrosion potential to obtain the corrosion current densities. Inhibition values were calculated from the I_{corr} values.

AC impedance measurements were carried out at E_{corr} immersion on standing in the atmosphere of air at the range from 1 to 10000 Hz at amplitude of 0.01 V. The impedance diagrams are given by Nyquist representation.

2.3 SEM Analysis

The specimens for surface morphological examination were immersed in an acid containing optimum concentration of inhibitor and blank for 2 h. Then, they were removed, rinsed quickly with acetone, and dried. The analysis was performed on Hitachi S 3000H Scanning Electron Microscope.

3. Result and Discussion

3.1 Weight Loss Study

The values of percentage inhibition efficiency (%IE) obtained from weight loss measurements for mild steel at different concentrations of plant extract in 1 M HCl at 300 K is summarized in Table 1. The variation of inhibition efficiency with increase in inhibitor concentrations is shown in Fig. 2. It was observed that the inhibitor inhibits the corrosion of mild steel in HCl solution, at all concentrations used in the study, i.e., 100-600 ppm. It is implicit that the inhibitor shows the highest inhibition efficiency (~97%) at 600 ppm in 1 M HCl.

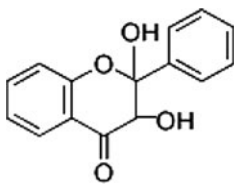

Fig. 1 Structure of 2,3-dihydroxyflavanone

Table 1 Variation of inhibition efficiency with different inhibitor concentrations

Concentration of inhibitor, ppm	IE, %
100	70.51
200	76.10
300	81.88
400	85.21
500	90.65
600	93.91

It is obvious from Fig. 1 and Table 1 that increase of inhibitor concentration increases the percentage of inhibition. It is clear that the inhibitor shows maximum inhibition of 96.45% at 600 ppm concentration. This suggests that increase in the inhibitor concentration increases the number of molecules adsorbed over the mild steel surface and blocks the active sites in which direct acid attack proceeds, and protects the metal from corrosion.

Table 2 and Fig. 3 represent the inhibition efficiency of the inhibitor at 600 ppm concentration in different acid concentrations. It is evident from the values that increase in concentration of acid decreases the inhibition efficiency of the inhibitor. The inhibitor shows highest inhibition efficiency in 1 M HCl. This is due to the increased aggressiveness of the acid solution.

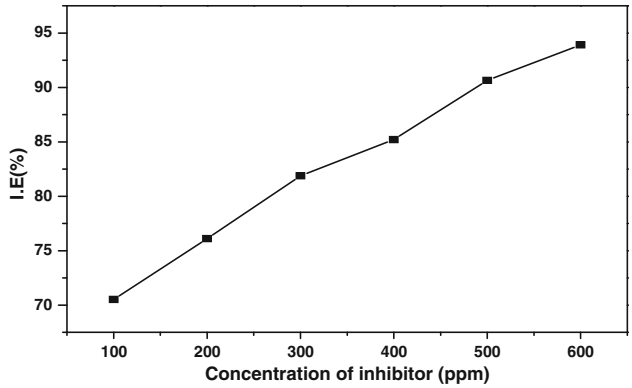

Fig. 2 Variation of inhibition efficiency with different inhibitor concentrations

Table 2 Variation of inhibition efficiency with different acid concentrations

Concentration of acid, M	IE, %
1	93.91
2	88.95
3	82.57
4	73.23

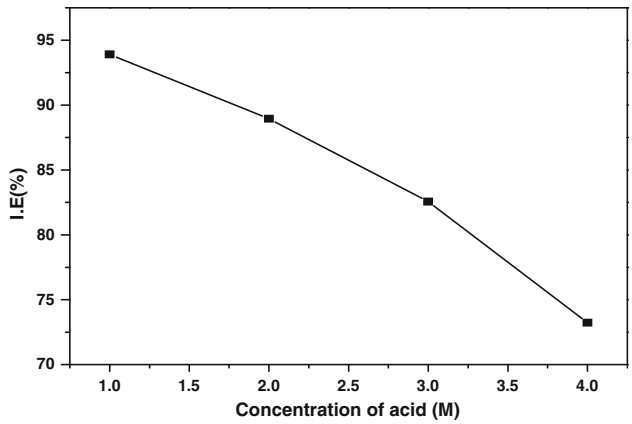

Fig. 3 Variation of inhibition efficiency with different acid concentrations

Table 3 Variation of inhibition efficiency with different immersion times

Immersion time, h	IE, %
2	93.91
3	94.16
4	94.47
5	94.88

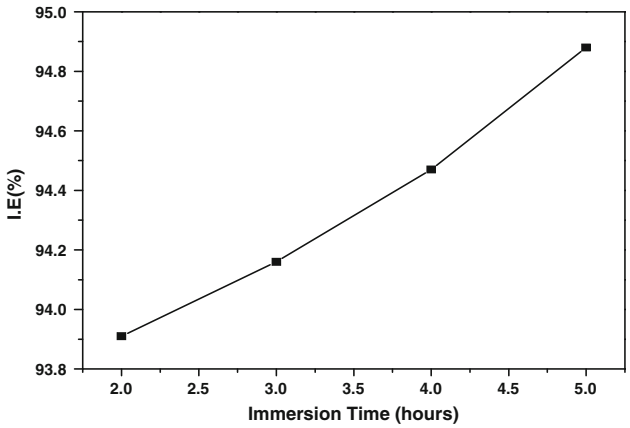

Fig. 4 Variation of inhibition efficiency with different immersion times

Table 4 Variation of inhibition efficiency with temperature

	IE, %					
T/*C*, K/ppm	100	200	300	400	500	600
300	70.51	76.10	81.88	85.21	90.65	93.91
310	66.10	71.99	75.85	80.55	86.95	89.56
320	60.98	66.85	69.79	76.18	80.16	82.79
330	54.69	59.91	65.13	69.98	74.59	76.22

T, temperature; C, concentration

Table 3 and Fig. 4 represent the inhibition efficiency of the inhibitor at 600 ppm concentration in 1 M HCl with different immersion times. It is very well clear from the table and the figure that when the immersion time increases the inhibition efficiency is also increased. This is due to stability and persistence of the adsorbed inhibitor layer on the metal surface.

Inhibition efficiencies of the inhibitor of 600 ppm concentration at different temperatures are shown in Table 4 and Fig. 5. It is observed from the table and figure that with increasing the temperature the inhibition efficiency decreases. The inhibitor shows maximum inhibition efficiency at 300 K. This gave a clue that the mechanism of adsorption of the inhibitor may be due to physisorption, because the physisorption is due to weak van der Waal's forces, which disappears at elevated temperatures.

3.2 Potentiodynamic Polarization studies

The potentiodynamic polarization curves of mild steel in absence and presence of various concentrations of the inhibitor

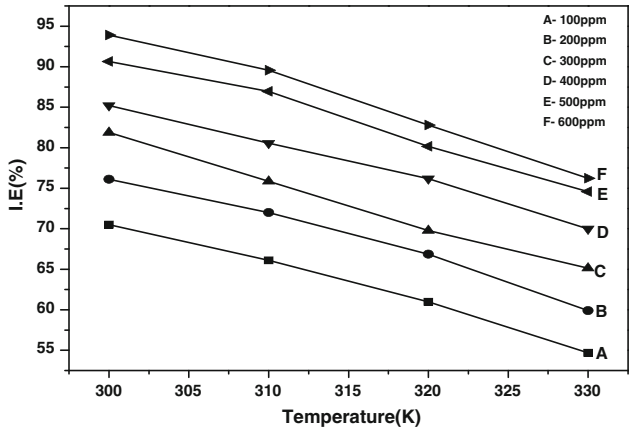

Fig. 5 Variation of inhibition efficiency with temperatures

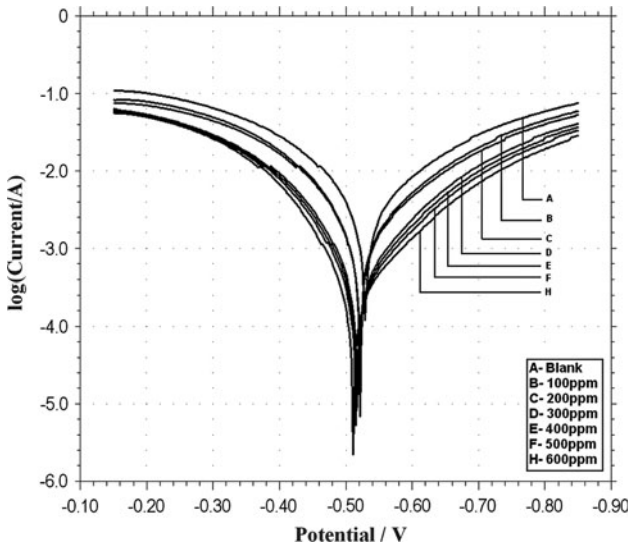

Fig. 6 Tafel polarization curves for mild steel in 1 M HCl in the presence and absence of inhibitor

Table 5 Tafel polarization parameter values for the corrosion of mild in the absence and presence of inhibitor in 1 M HCl

Concentration of inhibitor, ppm	I_{corr}, μA/cm^2	E_{corr}, mV vs. SCE	b_c, mV/decade	b_a, mV/decade	IE, %
0 (blank)	565.08	477	4.03	5.76	…
100	93.31	554	6.949	6.063	83.48
200	88.83	549	6.883	6.096	84.28
300	44.25	540	7.828	5.476	92.16
400	30.86	492	5.55	5.558	94.53
500	27.65	490	5.09	5.36	95.11
600	19.86	481	4.79	5.09	96.45

in 1 M HCl are shown in Fig. 6 and various electrochemical parameters such as corrosion potential (E_{corr}), corrosion current density (I_{corr}), percentage inhibition efficiency (%IE) and tafel constants (b_a and b_c) obtained from cathodic and anodic curves are given in Table 5. It is observed that the inhibitor suppressed

Table 6 Impedance parameter values for the corrosion of mild steel in 1 M HCl in presence and absence of inhibitor

Concentration of inhibitor, ppm	R_{ct}, Ω cm^2	C_{dl}, F/cm^2	IE, %
0 (blank)	16.19	0.002396	…
100	52.99	0.000113	69.45
200	70.689	0.000084	77.10
300	105.041	0.000056	84.59
400	129.551	0.000046	87.50
500	180.29	0.000039	91.02
600	269.89	0.000022	94.00

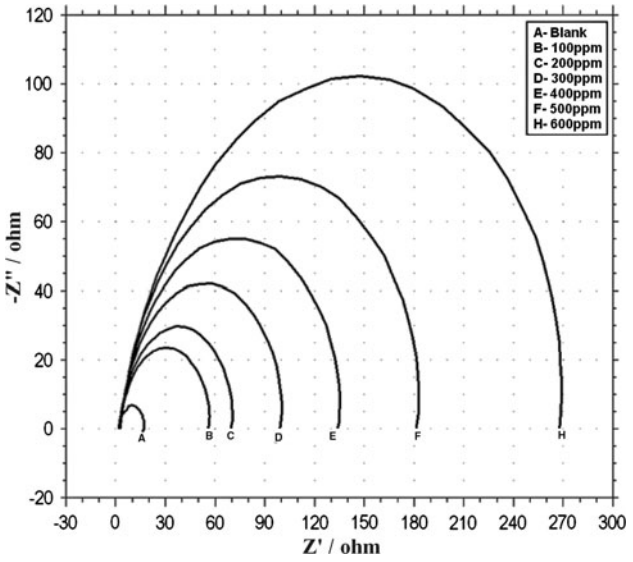

Fig. 7 Electrochemical impedance spectra of mild steel in 1 M HCl in the presence and absence of inhibitor

the cathodic reaction to greater extent than the anodic one at all concentrations. In other words, inhibitor under investigation predominantly inhibits cathodic than anodic corrosion.

3.3 Electrochemical Impedance Spectra Studies

Electrochemical impedance spectra for mild steel/1 M HCl interface in absence and presence of inhibitor were recorded in the frequency range 1 Hz to 10 kHz. The impedance data obtained were represented in Table 6 and Fig. 7. The Nyquist plots contain depressed semi-circle with the center under the real axis, whose size increases with the inhibitor indicating a charge transfer process mainly controlling the corrosion of mild steel. Such a behavior, characteristic for solid electrodes and often referred to as frequency dispersion that has been attributed to roughness and other inhomogeneities of the solid surface. It is apparent from these plots that the impedance response of mild steel in uninhibited acid solution has significantly changed after the addition of the inhibitor in the corrosion solutions. This indicated that the impedance of the inhibited substrate has increased with increasing concentration of inhibitor. The values of charge transfer resistance (R_{ct}) and double layer capacitance (C_{dl}) are obtained from Nyquist plot. The R_{ct} values increased with the increasing concentration of the inhibitor. On the other hand, the value of C_{dl} decreased with an increase in inhibitor concentration. This situation was the result of increase in the surface coverage by the inhibitor, which lead to an increase in the inhibition efficiency.

3.4 Adsorption Isotherms

The mechanism of corrosion inhibition may be explained on the basis of adsorption behavior. The degrees of surface coverage (θ) for different inhibitor concentrations were evaluated by weight loss data. Data were tested graphically by fitting to various isotherms. It is observed that plot obeys Langmuir adsorption isotherms through surface coverage of adsorbed inhibitor on mild steel surface and consequently, there is no interaction between the molecules adsorbed at the metal surface. The higher inhibitive property of the inhibitor is attributed due to the presence of π electrons, in oxygen and the larger molecular size, which insures greater coverage of the metallic surface.

Figure 8 shows Langmuir isotherm. The expected linear relationship is well approximated in Langmuir isotherm (correlation coefficient R^2 equal 0.9973), and the line has a slope of 1.2907 at 320 K. The deviation of the slope from unity is often interpreted as a sign that the adsorbing species occupy more or less than a typical adsorption site at the metal/solution interface.

Adsorption of the inhibitor molecule occurs because the interaction energy between the inhibitor and the metal surface. Basic information on the interaction between the inhibitor molecules and the surface of mild steel can be provided by adsorption isotherm. A correlation between surface coverage (θ) defined and the concentration of inhibitor (C_{inh}) in electrolyte can be represented by the Langmuir adsorption isotherm,

$$\frac{C_{inh}}{\theta} = \frac{1}{K} + C_{inh} \quad \text{(Eq 4)}$$

where K is the adsorption constant.

Surface coverage values (θ) for the inhibitor were obtained from the weight loss measurements for various concentrations at different temperatures (300-320 K), as shown in Table 7. The best-fitted straight line is obtained for the plot of C_{inh}/θ versus C_{inh} with slopes around unity. The correlation coefficient (r^2) was used to choose the isotherm that best fit experimental data. This suggests that the adsorption of inhibitor on metal surface followed the Langmuir adsorption isotherm (Fig. 8). From the intercepts of the straight lines C_{inh}/θ-axis, K values were calculated and are given in Table 7. The most important thermodynamic adsorption parameters are the free energy of adsorption (G_{ads}).The adsorption constant, K, is related to the standard free energy of adsorption, G_{ads}, with the following equation (Ref 16):

$$G_{ads} = -RT\ln(55.5K_{ads}) \quad \text{(Eq 5)}$$

where 55.5 is the water concentration of solution in mol/L.

The negative values of G_{ads} indicate the stability of the adsorbed layer on the steel surface and spontaneity of the adsorption process. The dependence of G_{ads} on temperature can be explained by two cases as follows:

(a) G_{ads} may increase (becomes less negative) with the increase of temperature which indicates the occurrence of exothermic process.

(b) G_{ads} may decrease (becomes more negative) with increasing temperature indicating the occurrence of endothermic process.

Generally, the magnitude of G_{ads} around −20 kJ/mol or less negative is assumed for electrostatic interactions exist between inhibitor and the charged metal surface (i.e., physisorption). Those around −40 kJ/mol or more negative are indication of charge sharing or transferring from organic species to the metal surface to form a coordinate type of metal bond (i.e., chemisorptions).

Inhibitor is free energy adsorption (G_{ads}) with temperature reveals that the inhibition of mild steel by inhibitor is an endothermic process. The free energy of adsorption (G_{ads}) for inhibitor around −30 kJ/mol. So, it can be classified as mixed-type inhibitor (Ref 16). The transition of metal/solution interface from a state of active dissolution to the passive state is attributed to the adsorption of the inhibitor molecules onto the metal surface, forming a protective film. Adsorption process can occur by electrostatic forces between ionic charges or dipoles of the adsorbed species and the electric charge on the metal surface. Also, the inhibitor molecules can be adsorbed onto the metal surface via the electron transfer from the adsorbed species to the vacant electron orbital of low energy in the metal to form a coordinate type of link. Therefore, the inhibitor absorption on the metal surface and thereby increasing the effectiveness of the corrosion inhibitor.

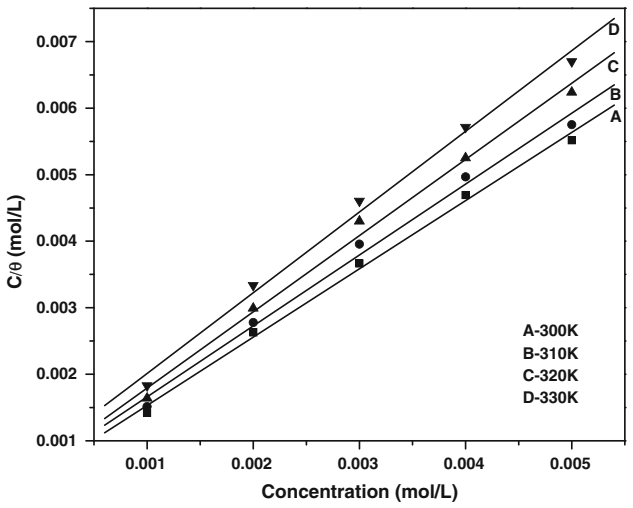

Fig. 8 Langmuir plot for inhibitor on mild steel in 1 M HCl at different temperatures

3.5 FT-IR Spectrum

FT-IR spectral studies were carried out for inhibitor and mild steel surface with inhibitor (Fig. 9) and their respective FT-IR peaks are given in Table 8. In Fig. 9(a), $\nu_{(C=O)}$, $\nu_{(O-C-O)}$, and $\nu_{(OH)}$ band are seen in these compounds, respectively, at 1687.00, 1139.83, and 3421.00 cm^{-1}.

In Fig. 9(b), the IR spectrum of the inhibitor adsorbed on the metal surface reveal the presence of functional group peaks whose absorption frequencies correspond to carbonyl C=O (shifted from 1687.00 to 1686.72 cm^{-1}), C-O-C (shifted from

Table 8 FT-IR peaks for the inhibitor and the adsorbed inhibitor on mild steel surface

Peaks from FT-IR spectra, cm^{-1}		
Inhibitor	**Mild steel**	**Functional group**
1687.00	1686.72	(C=0) stretch
1139.83	1124.36	(C-O-C) stretch
3421.00	3420.74	(OH) stretch

Table 7 Thermodynamic parameters for mild steel in 1 M HCl in the absence and presence of the inhibitor at different concentrations

Temperature, K	r^2	Slope	ΔG_{ads}, kJ/mol	K_{abs}, kJ/mol	ΔH_{ads}, kJ/mol	ΔS_{ads}, J/K · mol
300	0.9992	1.0863	−29.62	2.596×10^3	−15.044	−48.97
310	0.9988	1.1533	−30.39	2.384×10^3	−15.044	−48.97
320	0.9973	1.2907	−31.15	1.537×10^3	−15.044	−48.97

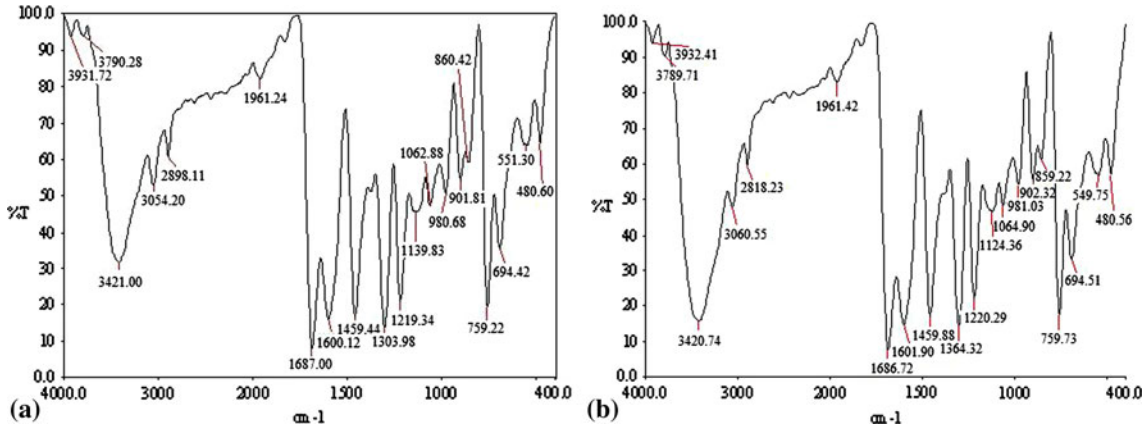

Fig. 9 (a) FT-IR spectrum of the inhibitor. (b) FT-IR spectrum of inhibitor adsorbed on metal surface

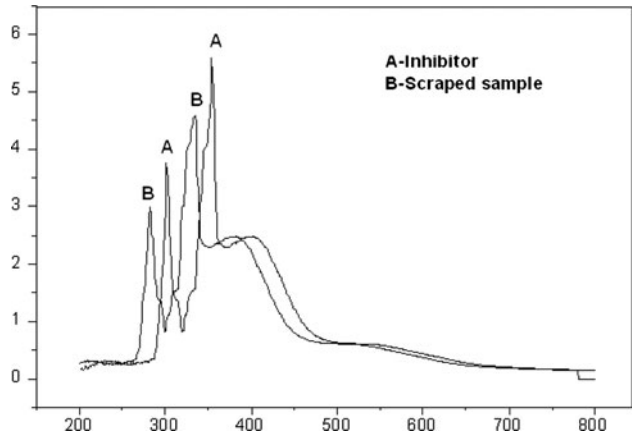

Fig. 10 UV-Vis spectra of (A) inhibitor and (B) inhibitor adsorbed on metal surface after 24 h

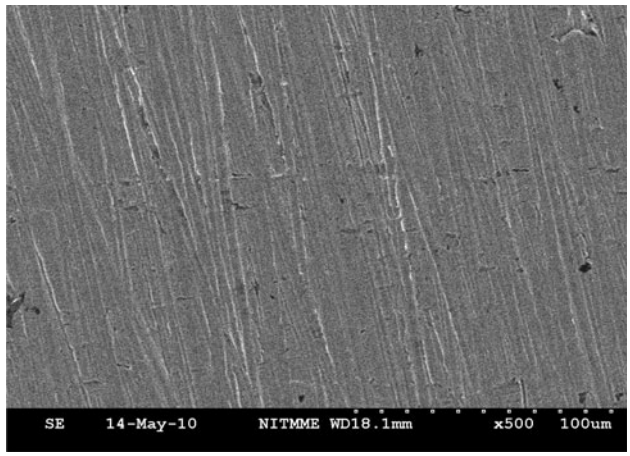

Fig. 11 SEM image of mild steel before immersion in 1 M HCl at 300 K (magnification, 500×)

1139.83 to 1124.36 cm^{-1}), and O-H (shifted from 3421.00 to 3420.74 cm^{-1}). The shift in the absorption frequencies of the inhibitor on the metal surface supports the interaction between the inhibitor and the metal surface. These changes in the absorption frequencies of IR spectra supported the interaction between functional group of inhibitor with surface of metal (Ref 17).

3.6 UV-Visible Spectrum

The absorption of monochromatic light is a suitable method for identification of complex ions. Change in position of the absorption maximum and or change in the value of absorbance indicate the formation of a complex between two species in solution. In order to confirm the possibility of the formation of inhibitor with Fe complex, UV-visible absorption spectra obtained inhibitor and after 24 h scrap inhibitor with mild steel are shown in Fig. 10. Bands at 275 and 325 nm are attributed to π to π* and *n* to π* transitions of carbonyl group which was present in inhibitor shown in Fig. 10 (curve A).

After 24 h of steel with inhibitor scrap sample Fig. 10 (curve B), it is clearly seen that the band in the region 354 nm, indicating that the carbonyl groups are held up in the complex with Fe. In the mean time, there is an increase in the absorbance of this band. These experimental findings give a strong evidence for the possibility of the formation of a complex between Fe^{2+} cation and inhibitor in 1 M HCl solution.

After 1 day of steel immersion, it is clearly seen that the band maximum of the *n*-π* and π-π* transition underwent a blue shift, indicating that the carbonyl groups are held up in the complex with Fe. In the mean time, there is an increase in the absorbance of this band (Ref 18).

3.7 SEM Analysis

The scanning electron microscope images were recorded to establish the interaction of organic molecules with the metal surface. Figure 11 to 13 shows SEM images of polished mild steel surface, mild steel immersed in 1 M HCl for 2 h, with and without inhibitor. The SEM images revealed that the specimens immersed in the inhibitor solutions are in better conditions having smooth surface, while the metal surface immersed in 1 M HCl is rough and covered with corrosion products and appeared like full of pits and cavities. This indicated that the

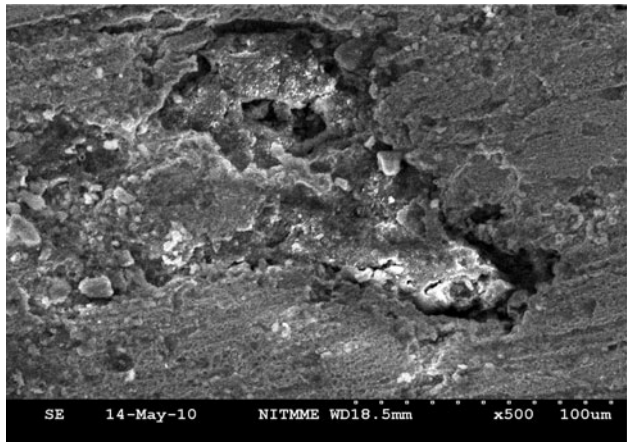

Fig. 12 SEM image of mild steel after 2 h immersion in 1 M HCl at 300 K (magnification 500×)

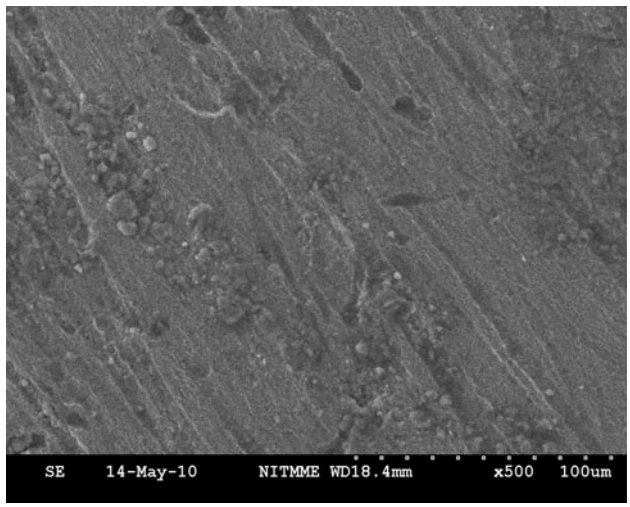

Fig. 13 SEM image of mild steel after immersion for 2 h in 1 M HCl in the presence of inhibitor at 300 K (magnification 500×)

inhibitor molecules hindered the dissolution of iron by forming organic film on the steel surface and there by reduced the rate of corrosion. Hence, the inhibitors protect mild steel in HCl solution.

4. Conclusion

The following are the conclusions drawn from this study:

1. The inhibition efficiency of the inhibitor increases with increase in inhibitor concentration, time and it is inversely proportional to the immersion time and temperature.
2. The inhibitor shows more than 96.45% of inhibition efficiency at 600 ppm concentration of inhibitor in 1 M HCl.
3. Langmuir provides evidence for both physisorption and chemisorption.
4. From the polarization studies, it is evident that 2,3-dihydroxyflavanone acts as a mixed type inhibitor.
5. Impedance measurements revealed the increase of charge transfer resistance and decrease of double layer capacitance with increase in the concentration of inhibitor.
6. SEM image was taken for blank acid corroded plate and inhibitor plate. The surface of blank plate has crevices but the inhibitor surface was smooth.
7. As a final point, the inhibitor is good for hydrochloric acid corrosion on mild steel.

References

1. S.S. Abd El Rehim, M.A.M. Ibrahim, and K.F. Khalid, The Inhibition of 4-(2′-amino-5′- methylphenylazo) Antipyrine on Corrosion of Mild Steel in HCl Solution, *Mater. Chem. Phys.*, 2001, **70**, p 268–273
2. E.E. Oguzie, C. Unaegbu, C.N. Ogukwe, B.N. Okolue, and A.I. Onuchukwu, Inhibition of Mild Steel Corrosion in Sulphuric Acid Using Indigo Dye and Synergistic Halide Additives, *Mater. Chem. Phys*., 2004, **84**, p 363–368
3. F. Bentiss, M. Lebrini, and M. Lagrene, Thermodynamic Characterization of Metal Dissolution and Inhibitor Adsorption Processes in Mild Steel/2,5-bis(n-thienyl)-1,3,4-thiadiazoles/Hydrochloric Acid System, *Corros. Sci.*, 2005, **47**, p 2915–2931
4. M. Lebrini, F. Bentiss, H. Vezin, and M. Lagrenée, Inhibitive Properties, Adsorption and a Theoretical Study of 3,5-bis(n-pyridyl)-4-amino-1,2,4-triazoles as Corrosion Inhibitors for Mild Steel in Perchloric Acid, *Appl. Surf. Sci.*, 2005, **252**, p 950
5. S.A. Ali, A.M. El-Shareef, R.F. Al-Ghamdi, and M.T. Saeed, The Isoxazolidines: The Effects of Steric Factor and Hydrophobic Chain Length on the Corrosion Inhibition of Mild Steel in Acidic Medium, *Corros. Sci.*, 2005, **47**, p 2659–2678
6. M.A. Migahed, Electrochemical Investigation of the Corrosion Behaviour of Mild Steel in 2 M HCl Solution in Presence of 1-Dodecyl-4-methoxy pyridinium Bromide, *Mater. Chem. Phys.*, 2005, **93**, p 48–53
7. E.E. Oguzie, Corrosion Inhibition of Aluminium in Acidic and Alkaline Media by *Sansevieria trifasciata* Extract, *Mater. Lett.*, 2005, **59**, p 1076
8. E.A. Noor, The Inhibition of Mild Steel Corrosion in Phosphoric Acid Solutions by Some N-Heterocyclic Compounds in the Salt Form, *Corros. Sci.*, 2005, **47**, p 33–55
9. A.Y.E. Etre, M. Abdullah, and Z.E.E. Tantawy, Corrosion Inhibition of Some Metals Using Lawsonia Extract, *Corros. Sci.*, 2005, **47**, p 385–395
10. C.A. Loto, A.I. Mohammed, and R.O. Loto, Inhibition Evaluation of Mango Juice Extracts on the Corrosion of Mild Steel in HCl, *Corros. Prev. Control*, 2003, **50**, p 107
11. S. Rajendran, S. Shanmugapriya, T. Rajalakshmi, and A.J. Amalraj, Corrosion Behaviour of Aluminium in the Presence of an Aqueous Extract of *Hibiscus rosasinensis*, *Corros. Sci.*, 2005, **61**, p 685
12. M. Hosseini, F.L. Metrtens, M. Ghorbani, and R. Mohammed Arshadi, Asymmetrical Schiff Bases as Inhibitors of Mild Steel Corrosion in Sulphuric Acid Media, *Mater. Chem. Phys.*, 2003, **78**, p 800–808
13. M. Lavanya, D. Kesavan, N. Prabhavathi, and N. Sulochana, Studies on the Inhibitive Effect of 3-Hydroxyflavone on the Acid Corrosion of Mild Steel, *Surf. Rev. Lett.*, 2009, **16**, p 845
14. M.G. Sethuraman and P.B. Raja, Corrosion Inhibition of Mild Steel by Datura Metel, *Pigment Resin Technol.*, 2005, **34**, p 327
15. M.A. Quraishi, I. Ahamad, A.K. Singh, S. Shukla, B. Lal, and V. Singh, *N*-(Piperidinomethyl)-3-[(pyridylidene) amino]isatin: A New and Effective Acid Corrosion Inhibitor for Mild Steel, *Mater. Chem. Phys*., 2008, **112**, p 1035–1039
16. P. Kalaiselvi, S. Chellammal, S. Palanichamy, and G. Subramanian, *Artemisia pallens* as Corrosion Inhibitor for Mild Steel in HCl Medium, *Mater. Chem. Phys.*, 2010, **120**, p 643–648
17. S. K. Rajappa, T. V. Venkatesha, and B. M. Praveen, *Chemical treatment of zinc surface and its corrosion inhibition studies,* Indian Academy of Sciences, 2008, p 37-41
18. Y. Abbouda, A. Abourriche, T. Saffaj, M. Berrada, M. Charrouf, A. Bennamara, N.A.L. Himidi, and H. Hannache, A Novel Azo Dye, 8-Quinolinol-5-Azoantipyrine as Corrosion Inhibitor for Mild Steel in Acidic Media, *Mater. Chem. Phys.*, 2005, **105**, p 1–5